Magnetic phases near the Van Hove singularity in *s*- and *d*-band Hubbard models

Marcus Fleck, Andrzej M. Oleś,* and Lars Hedin
Max-Planck-Institut für Festkörperforschung, Heisenbergstrasse 1, D-70569 Stuttgart, Germany
(Received 21 March 1997)

We investigate the magnetic instabilities of the nondegenerate (*s*-band) and a degenerate (*d*-band) Hubbard model in two dimensions using many-body effects due to particle-particle diagrams and Hund's rule local correlations. The density of states and the position of the Van Hove singularity change depending on the value of next-nearest-neighbor hopping t'. The Stoner parameter is strongly reduced in the *s*-band case, and ferromagnetism survives only if the electron density is small and the band has flat regions. Due to next-nearest-neighbor hopping there are flat regions in Γ-X and Γ-Y directions. In contrast, for the *d*-band case the reduction of the Stoner parameter which follows from particle-particle correlations is much smaller and ferromagnetism survives to a large extent. Inclusion of local spin-spin correlations has a limited destabilizing effect on the magnetic states. [S0163-1829(97)00330-5]

I. INTRODUCTION

Although efforts to understand the microscopic origin of itinerant magnetism have continued for over three decades, there is still no consensus whether the nondegenerate (*s*-band) Hubbard model, originally introduced as a model for *d* electrons in transition metals,[1] can serve as a simple model which describes itinerant ferromagnetism. On the mean-field level it seems to be a good starting point as the Stoner criterion predicts a ferromagnetic (FM) ground state (g.s.) in a broad range of parameters. However, the inclusion of electron correlations destabilizes it in most situations.[1–5] However, the FM state is stable in the limit of $U\rightarrow\infty$ up to a critical doping, being close to $\delta=0.29$ for a square lattice.[4,5] Recently, a few mechanisms which stabilize ferromagnetism in the Hubbard model with moderate Coulomb repulsion U have been proposed. They are realized either by extending the model by additional intersite Coulomb interactions[6] or in the flat-band scenario.[7–12] While the former mechanism might work in liquid hydrogen rather than in transition metals,[6] the question of whether the spin-independent on-site Coulomb interaction U alone can give ferromagnetism remains intriguing.

Rather extreme situations in which the g.s. is FM are encountered in low-dimensional systems. First, high-spin g.s.'s are found in finite systems with open-shell electronic states, like in a tetrahedron,[13] and in some other few-atom clusters.[14] Second, the enhanced degeneracy at the Fermi level realized in one dimension by extended hopping stabilizes the FM g.s.[8–12] The mean-field analysis of Lin and Hirsch[7] suggests that the FM instability is enhanced in two dimensions by the next-nearest-neighbor hopping t', and indeed the summation of the most divergent diagrams confirms the FM instability at the Van Hove singularity (VHS) in two dimensions.[15] There are also indications from the enhanced stability of the Nagaoka state by t' at the $U=\infty$ limit that the kinetic energy changing slowly with electron filling favors ferromagnetism in a square lattice.[16]

Yet in spite of this revived interest in the magnetic states of the nondegenerate Hubbard model, magnetic states are realized in nature in degenerate *d* bands of 3*d* transition metals. Therefore, we investigate here the FM and antiferromagnetic (AFM) instabilities of the *d* band and compare them with those found in the *s* band for the same two-dimensional (2D) lattice near the VHS. It is important to include electron correlations, if magnetic instabilities are considered. Using the Kadanoff-Baym technique of deriving conserving approximations, we find by including particle-particle scattering a similar expression as postulated and used by Chen *et al.* in the *s*-band case.[17] Note that this approach is different from fluctuation exchange approximation (FLEX),[18,19] and avoids self-consistency in the conserving approximation, but nevertheless gives a magnetic structure factor of the same quality as the Monte Carlo simulations in 2D (Refs. 17 and 20) and in infinite-dimensional Hubbard models.[21] In contrast, the experimental data suggest that the Hund's rule exchange interaction J remains practically equal to its atomic value,[22] but the *atomic correlations* stabilize local moments for $J>0$. In the Hartree-Fock (HF) approximation these moments exist only in the symmetry-broken phases, and they are absent in nonmagnetic states.[23] Thus, both particle-particle scattering and atomic correlations contribute to the reduction of the magnetic energy in the *d* band, conventionally expressed by the Stoner parameter I_d. This motivated us to make a more extended study, in which we analyze the FM and AFM instabilities and discuss two questions: (i) Does ferromagnetism exist in the *s*-band model in a finite-density range near the VHS? If it does, it might be possible to stabilize it also in three dimensions, provided a high density of states would exist at the Fermi level. (ii) How does the picture change when we go to the *d*-band case?

The paper starts with the presentation of *s*-band and *d*-band Hubbard models with next-nearest-neighbor hopping in Sec. II. The *d*-band case is treated by a generalization of the treatment of the particle-particle scattering presented in Ref. 17. We also include atomic spin-spin correlations by a local ansatz method and evaluate the renormalized Stoner parameters. The magnetic phase diagrams of the *s* and *d* bands are presented and discussed in Sec. III. The paper is concluded in Sec. IV, where we also give estimations of the parameters used for realistic transition metals.

II. MODELS AND RENORMALIZED STONER PARAMETERS

First, we consider a nondegenerate Hubbard (s-band) model on a square lattice with nearest ($t>0$) and next-nearest neighbor ($t'>0$) hopping,[7]

$$H_s=-t\sum_{\langle ij\rangle,\sigma} c_{i\sigma}^{\dagger}c_{j\sigma}+t'\sum_{\langle\langle ij\rangle\rangle,\sigma} c_{i\sigma}^{\dagger}c_{j\sigma}+U\sum_i n_{i\uparrow}n_{i\downarrow}\,. \tag{1}$$

An increasing t' makes the kinetic energy

$$\varepsilon_{\mathbf{k}}=-2t(\cos k_x+\cos k_y)+4t'\cos k_x\cos k_y \tag{2}$$

to increase slower from the Γ to the $X(Y)$ point, and finally to become flat for $R=1$, where $R=2t'/t$. We do not consider the unrealistic cases with large $R>1$. Second, we study a degenerate d-band model, with a simplified intraorbital hopping,[24]

$$\begin{aligned}H_d=&-t\sum_{\langle i,j\rangle,\alpha,\sigma} c_{i\alpha,\sigma}^{\dagger}c_{j\alpha,\sigma}+t'\sum_{\langle\langle i,j\rangle\rangle,\alpha,\sigma} c_{i\alpha,\sigma}^{\dagger}c_{j\alpha,\sigma}\\&+U_0\sum_{i,\alpha} n_{i\alpha,\uparrow}n_{i\alpha,\downarrow}+\left(U-\frac{J}{2}\right)\sum_{i,\alpha<\beta} n_{i\alpha}n_{i\beta}\\&-2J\sum_{i,\alpha<\beta}\mathbf{S}_{i\alpha}\cdot\mathbf{S}_{i\beta}+J\sum_{i,\alpha\neq\beta} c_{i\alpha,\uparrow}^{\dagger}c_{i\alpha,\downarrow}^{\dagger}c_{i\beta,\downarrow}c_{i\beta,\uparrow}\,,\end{aligned} \tag{3}$$

where $n_{i\alpha}=\Sigma_\sigma n_{i\alpha,\sigma}$ and $\mathbf{S}_{i\alpha}=\{S_{i\alpha}^x,S_{i\alpha}^y,S_{i\alpha}^z\}$ are density and spin operators for orbital α at site i, and $U_0=U+2J$. The d bands have the same dispersion $\varepsilon_{\mathbf{k}}$ as in the s-band model (1).

Following the approach of Kadanoff and Baym,[25] one may construct a ''conserving approximation'' to the d-band Hubbard model which motivates the approach of Chen *et al.*[17] Therefore, we have considered a system coupled to an infinitesimal external field $\mathbf{b}_{i\alpha}=(b_{i\alpha}^x,b_{i\alpha}^y,b_{i\alpha}^z)$,

$$H_d(\mathbf{b})=H_d-\sum_{i\alpha}\mathbf{b}_{i\alpha}\cdot\mathbf{S}_{i\alpha}\,, \tag{4}$$

and derived a self-energy by taking the functional derivative with respect to the full Green function G of the Kadanoff-Baym potential Φ, $\Sigma=\delta\Phi/\delta G$. In a finite field $\mathbf{b}_{i\alpha}$ one finds the Dyson equation for the one-particle Green function of the d-band Hamiltonian (4),

$$\hat{G}_{ij,\alpha}^{-1}(\tau)=\hat{G}_{ij,\alpha}^{0-1}(\tau)-\hat{\Sigma}_{ij,\alpha}(\tau)+\mathbf{b}_{i\alpha}\cdot\hat{\boldsymbol{\sigma}}\,\delta(\tau)\,\delta_{i,j}, \tag{5}$$

where $\hat{G}_{ij,\alpha}^0$ is the noninteracting (i.e., $U=J=0$) (diagonal) Green function matrix, $\hat{\Sigma}_{ij,\alpha}$ is the (nondiagonal) self-energy matrix labeled by spin indices, and $\hat{\boldsymbol{\sigma}}$ is a vector composed out of Pauli matrices. Due to the symmetry of the hypercubic lattice considered here, there are no interorbital hopping processes, and therefore the one-particle Green function $\hat{G}_{ij,\alpha}(\tau)$ is diagonal in orbital space.

The magnetic instabilities follow from the instabilities of the linear response function (the transverse susceptibility) to a local spin-flip excitation ($b_{i\alpha}^-=b_{i\alpha}^x-ib_{i\alpha}^y$),

$$\chi_{ij,\alpha}^{\perp}(\tau-\tau')=\lim_{\epsilon\to 0^+}\sum_{\beta}\left.\frac{\partial G_{jj,\alpha}^{\uparrow\downarrow}(\tau',\tau'+\epsilon)}{\partial b_{i,\beta}^-(\tau)}\right|_{\mathbf{b}=0}, \tag{6}$$

which is determined by the full one-particle Green function G. Using a well-known identity we rewrite the functional derivative as

$$\begin{aligned}&\left.\frac{\partial\hat{G}_{jj,\alpha}(\tau',\tau'+\epsilon)}{\partial b_{i,\beta}^-(\tau)}\right|_{\mathbf{b}=0}\\&\quad=-\int\hat{G}_{ji_1,\alpha}(\tau',\tau_{i_1})\frac{\partial\hat{G}_{i_1i_2,\alpha}^{-1}(\tau_{i_1},\tau_{i_2})}{\partial b_{i,\beta}^-(\tau)}\\&\qquad\times\hat{G}_{i_2j,\alpha}(\tau_{i_2},\tau'+\epsilon)_{\mathbf{b}=0},\end{aligned} \tag{7}$$

where $\int\equiv\Sigma_{i_\eta}\int d\tau_{i_\eta}$ stands for integration and summation over all internal variables $\{i_\eta\}$. Using the Dyson equation (5), we find a formal integral equation for the transverse susceptibility,

$$\begin{aligned}\chi_{ij,\alpha}^{\perp}(\tau-\tau')=\chi_{ij,\alpha}^{\perp 0}(\tau-\tau')+\sum_{\beta}\int\mathrm{Tr}[&\hat{\sigma}^-\hat{G}_{ji_1,\alpha}(\tau',\tau_{i_1})\\&\times\Gamma_{\alpha\beta}(i_1\tau_{i_1},i_2\tau_{i_2}|i_3\tau_{i_3})\hat{G}_{i_2j,\alpha}(\tau_{i_2},\tau')]\\&\times\chi_{ii_3,\beta}^{\perp}(\tau-\tau_{i_3})|_{\mathbf{b}=0},\end{aligned} \tag{8}$$

where $\hat{\sigma}^-=\hat{\sigma}^x-i\hat{\sigma}^y$ is a Pauli matrix, and the *effective two particle* interaction is defined as

$$\Gamma_{\alpha\beta}(i_1\tau_{i_1},i_2\tau_{i_2}|i_3\tau_{i_3})\equiv\lim_{\epsilon\to 0^+}\frac{\partial\hat{\Sigma}_{i_1i_2,\alpha}(\tau_{i_1},\tau_{i_2})}{\partial G_{i_3i_3,\beta}^{\uparrow\downarrow}(\tau_{i_3},\tau_{i_3}+\epsilon)}. \tag{9}$$

One observes immediately that a random-phase-approximation- (RPA) like expression for the transverse susceptibility would be obtained, if the self-energy $\hat{\Sigma}_{ij,\alpha}(\tau)$ were local in space and time, as is, e.g., the HF self-energy.

We will now use the Kadanoff-Baym technique which may be used to obtain conserving approximations.[25] First, we rewrite the expression for H_d, Eq. (3), in a more explicit form which separates the spin-spin interaction into transverse and longitudinal terms,

$$\begin{aligned}H_d=&-t\sum_{\langle i,j\rangle,\alpha,\sigma} c_{i\alpha,\sigma}^{\dagger}c_{j\alpha,\sigma}+t'\sum_{\langle\langle i,j\rangle\rangle,\alpha,\sigma} c_{i\alpha,\sigma}^{\dagger}c_{j\alpha,\sigma}\\&+U_0\sum_{i\alpha} n_{i\alpha\uparrow}n_{i\alpha\downarrow}-J\sum_{i,\alpha<\beta,\sigma} c_{i\alpha,\sigma}^{\dagger}c_{i\alpha,-\sigma}c_{i\beta,-\sigma}^{\dagger}c_{i\beta,\sigma}\\&+\sum_{i,\alpha<\beta,\sigma}[Un_{i\alpha,\sigma}n_{i\beta,-\sigma}+(U-J)n_{i\alpha,\sigma}n_{i\beta,\sigma}]\\&+J\sum_{i,\alpha\neq\beta} c_{i\alpha,\uparrow}^{\dagger}c_{i\alpha,\downarrow}^{\dagger}c_{i\beta,\downarrow}c_{i\beta,\uparrow}\,.\end{aligned} \tag{10}$$

The diagrams to lowest order in the Kadanoff-Baym functional Φ (see Fig. 1) are obtained by taking the g.s. expec-

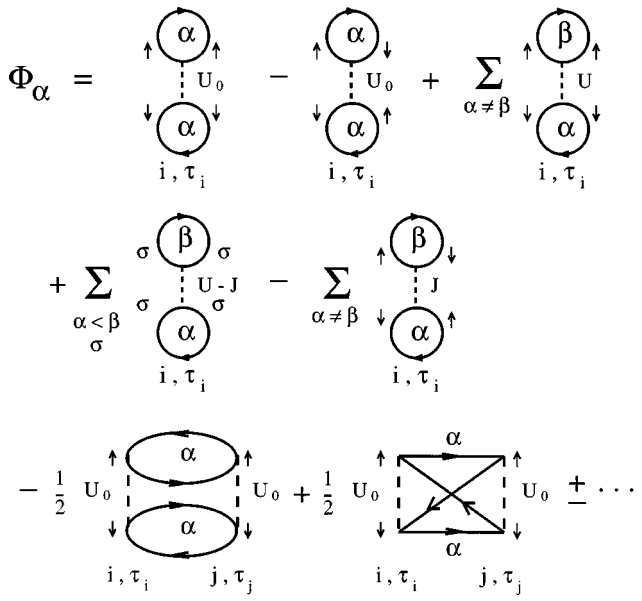

FIG. 1. Schematic representation of the diagrammatic expansion of the Kadanoff-Baym potential part which originates from electron-electron interaction with a representative d orbital, Φ_α. The first- and second-order diagrams are shown; higher-order diagrams include multiple particle-particle scattering and dress the intraorbital Coulomb interaction U_0 further.

tation values of all possible contractions of the operators in H_d. Since we have a spin-flip term due to the infinitesimal field $\mathbf{b}_{i\alpha}$, also spin-flip Green functions appear. In choosing higher-order terms, we have only kept diagrams corresponding to particle-particle scattering, similarly as in the FLEX method in Ref. 19.

For Kadanoff-Baym diagrams we only keep those which contribute both to the Green function and to the susceptibility. In this way we avoid inconsistencies when we calculate phase boundaries from total energy, using the Green function, and from finding singularities in the susceptibility. This means that we only keep diagrams of second order in $\langle c^\dagger_{i\alpha,\sigma} c_{i\beta,\sigma'}\rangle$, since diagrams of higher and lower order give vanishing contributions when we take the two functional derivatives and the limit of zero external field, $\mathbf{b}_{i\alpha}\to 0$. The leading diagrams of a consistent theory are shown in Fig. 1. The generating functional for the self-energy is obtained by summing up to infinite order the class of diagrams in the particle-particle channel, which leads to an alternating geometric series, shown in Fig. 1. One then integrates over all internal variables and sums over orbitals, $\Phi=\Sigma_\alpha \int \Phi_\alpha$.

Short-range electron-electron correlation effects, neglected within the RPA, consist of local particle-particle scattering processes. Here we use a *local approximation*, and thus the contribution of each higher-order diagram to Φ_α is $\propto \delta_{i,j}$.

Compared to other dynamical electronic processes, particle-particle scattering can be considered as instantaneous process. Focusing on the local particle-particle kernel $\chi^{pp}_{ii,\alpha}(\tau_i-\tau_j)=G^{\uparrow\uparrow}_{ii,\alpha}(\tau_i-\tau_j)G^{\downarrow\downarrow}_{ii,\alpha}(\tau_i-\tau_j)$, shown in the second-order diagrams of Fig. 1, it is reasonable to write $\chi^{pp}_{ii,\alpha}(\tau_i-\tau_j)\approx\chi^{pp}_{ii,\alpha}(\omega=0)\,\delta(\tau_i-\tau_j)$, where

$$\chi^{pp}_{ii,\alpha}(0)=\frac{1}{\beta}\sum_n G^{\uparrow\uparrow}_{ii,\alpha}(i\omega_n)G^{\downarrow\downarrow}_{ii,\alpha}(-i\omega_n), \tag{11}$$

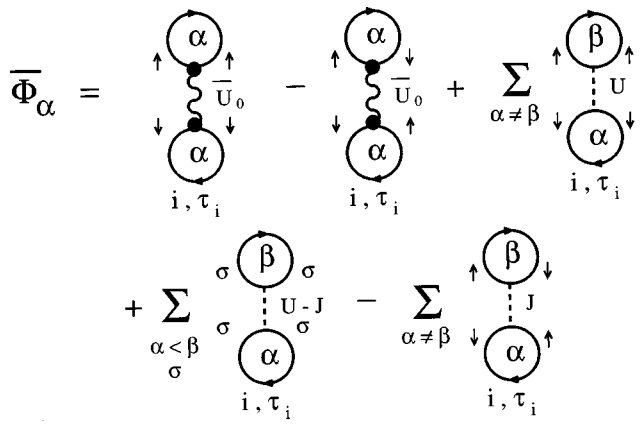

FIG. 2. Schematic representation of the diagrammatic expansion of the effective Kadanoff-Baym potential $\overline{\Phi}_\alpha$ with the effective intraorbital Coulomb interaction $\overline{U_0}$, defined by Eq. (13).

with $\beta=1/k_BT$. Within this approximation one may replace the interaction between two electrons in $|\alpha\uparrow\rangle$ and $|\alpha\downarrow\rangle$ states, shown by higher-order diagrams in Fig. 1, by the effective interaction $\overline{U_0}$, and we can map Φ onto an effective Kadanoff-Baym potential $\overline{\Phi}=\Sigma_\alpha\int\overline{\Phi}_\alpha$, shown by its diagrammatic representation in Fig. 2. The interaction vertex in the effective Kadanoff-Baym potential obeys the equation

$$\overline{U_0}=U_0-U_0\chi^{pp}_\alpha(0)\overline{U_0}, \tag{12}$$

where $\chi^{pp}_\alpha(0)=\chi^{pp}_{ii,\alpha}(0)$ for a translationally invariant system, which is easily solved to give an effective intraorbital Coulomb interaction in the d band,

$$\overline{U_0}=\frac{U_0}{1+U_0\chi^{pp}_\alpha(0)}. \tag{13}$$

It is now straightforward to calculate the self-energy in the one-particle Green function. Performing explicitly the functional derivatives, $\Sigma=\delta\Phi/\delta G$, we find the local self-energy matrix

$$\hat{\Sigma}_{ij,\alpha}(\tau-\tau')=\begin{pmatrix}\Sigma^{\uparrow\uparrow}_{i\alpha} & \Sigma^{\uparrow\downarrow}_{i\alpha}\\ \Sigma^{\uparrow\downarrow *}_{i\alpha} & \Sigma^{\downarrow\downarrow}_{i\alpha}\end{pmatrix}\delta(\tau-\tau')\,\delta_{i,j}, \tag{14}$$

with elements

$$\Sigma^{\sigma\sigma}_{i\alpha}=\left[\overline{U_0}\langle n_{i\alpha,-\sigma}\rangle+\sum_{\beta\neq\alpha}\left(U\langle n_{i\beta}\rangle-J\langle n_{i\beta,-\sigma}\rangle\right)\right],$$

$$\Sigma^{\uparrow\downarrow}_{i\alpha}=-\left[\overline{U_0}\langle S^-_{i\alpha}\rangle-J\sum_{\beta\neq\alpha}\langle S^-_{i\beta}\rangle\right]. \tag{15}$$

The adopted approximation to the self-energy has the same functional form as the usual Hartree-Fock approximation, and therefore we call it a generalized HF (GHF) approximation. Self-consistency for the presented Φ-derivable GHF approximation is required only for the GHF occupation numbers $\langle n_{i\alpha,\sigma}\rangle$.

Next, a RPA-like expression for the transverse susceptibility is obtained, using the Green function with the self-energy, Eq. (15), in Eqs. (9) and (8),

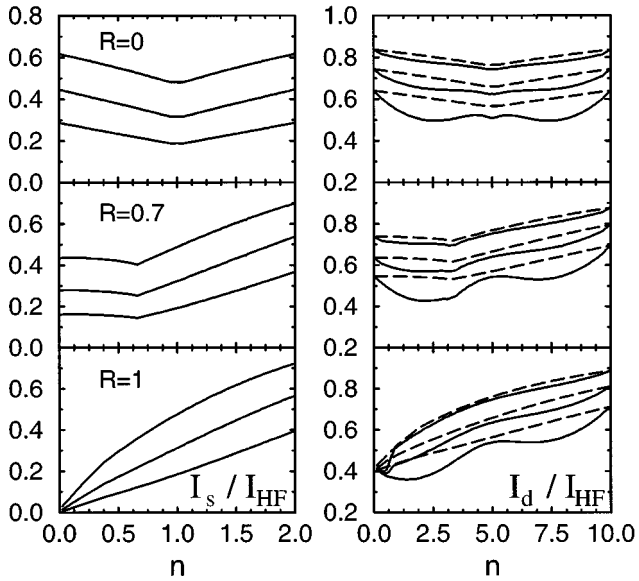

FIG. 3. Stoner parameters $I_s/I_{\rm HF}$ for the s band (left) and $I_d/I_{\rm HF}$ for the d band (right) as a function of filling for different R values. The three solid curves in each panel refer to $(U+6J)/W=0.5$, 1.0, and 2.0 from top to bottom. The dashed curves in the d-band case are results with spin-spin correlations (from the local ansatz) included.

$$\chi^{\perp}_{\alpha}(\mathbf{q},0)=\frac{\chi^{0}_{\alpha}(\mathbf{q},0)}{1-I_d\chi^{0}_{\alpha}(\mathbf{q},0)}, \tag{16}$$

which we will call generalized RPA (GRPA), since it has the same functional form as in the RPA. In the s-band case the above formula contains $I_s=\overline{U}$ (instead of I_d), where $\overline{U}$ is defined by the same renormalization due to the particle-particle vertex as in Eq. (12), but with U_0 replaced by U, and gives an excellent agreement with the Monte Carlo data.[17] There seems no reason that this approximation should not work well also in the d-band case.

As an important difference to the RPA, the HF value of the Stoner parameter for the d-band model, $I_{\rm HF}=(U+6J)/5$, is now replaced by the renormalized Stoner parameter

$$I_d=\tfrac{1}{5}(\overline{U_0}+4J). \tag{17}$$

We note that the Stoner parameter in the s band is just equivalent to the renormalized value of U, $I_s=\overline{U}$.

The reduction of the Stoner parameter due to the screening of the intraorbital Coulomb interaction U_0 may be substantial in a d band, but not quite as large as in the s-band case, as we show below. In contrast, the screening of the exchange interaction J is provided by similar expressions which involve the interorbital transitions on the same site, $G^{\sigma\sigma}_{i\alpha,i\beta}$, and is thus of second order in $\langle c^{\dagger}_{i\alpha,\sigma}c_{i\beta,\sigma}\rangle$. If the interorbital hopping vanishes (as it does for hypercubic lattices), J is unscreened; otherwise, this screening is expected to be small. This is confirmed by the values of J deduced from the experimental data in transition metals which are close to the atomic values.[22] We note that the renormalization of I_d is therefore substantially weaker than in the s-band Hubbard model (1) (Fig. 3), where $I_s=\overline{U}$, and $\overline{U}$ is obtained from Eq. (12) with $J=0$. In the 2D Hubbard model one finds that I_s is only weakly dependent on the band filling n, with a minimum at the filling which corresponds to the VHS, but is *finite* as long as $R<1$. With increasing R, the VHS moves towards the lower band edge, the reduction of I_s gets stronger, and one finds that $I_s\to 0$ for $R\to 1$. Such a strong renormalization of I_s follows from the singular behavior of the particle-particle vertex.

The Stoner parameter is further decreased in the d-band case by atomic interorbital correlations.[23] This results from the formation of local moments which can be built into the g.s. by modifying a single-Slater-determinant HF wave function $|\Psi_{\rm HF}\rangle$ into[26]

$$|\Psi_0(\{n_{i\alpha,\sigma}\})\rangle=\exp\Big(-\sum_m \eta_m O_m\Big)|\Psi_{\rm HF}(\{n_{i\alpha,\sigma}\})\rangle, \tag{18}$$

where η_m are variational parameters, and O_m are local operators which in the case of a d band have the form

$$O^{(n)}_{i,\alpha\beta}=n_{i\alpha}n_{i\beta}, \quad O^{(s)}_{i,\alpha\beta}=\mathbf{S}_{i\alpha}\cdot\mathbf{S}_{i\beta}, \tag{19}$$

and describe local density ($O^{(n)}_{i,\alpha\beta}$) and spin ($O^{(s)}_{i,\alpha\beta}$) correlations, respectively. The contribution of spin correlations to the magnetic energy follows from a comparison of the energy obtained with the wave function $|\Psi_0(\{n_{i\alpha,\sigma}\})\rangle$ given by Eq. (18) with that found with density correlations only.[23] We note that the HF and correlated wave functions in Eq. (18) are obtained for the same electronic distribution. The Stoner parameter I_d is obtained as a derivative of the interaction energy with respect to magnetization squared, and is additionally reduced by up to 12% of I_d, if $(U+6J)/W=1$ (Fig. 3). Therefore, one finds at $(U+6J)/W=1$ that $I_d/I_{\rm HF}\simeq 0.65$ which agrees well with the values deduced within a realistic model for $3d$ transition metals.[27] Interestingly, at $R=0$ the largest corrections due to spin-spin correlations are found at $|n-5|\simeq 2.5$, which indicates that the difference between local moments in the paramagnetic (PM) and weakly FM states is there larger than at $n=5$.[28]

III. MAGNETIC PHASE DIAGRAMS

The instability of the system towards either FM or AFM order (16) is driven by the value of the Stoner parameter I_d (I_s). We illustrate this by considering the phases with a uniform and with a two-sublattice magnetic structure,[29]

$$\langle n_{i\alpha,\sigma}\rangle=\tfrac{1}{2}[n_0+\lambda_\sigma m+(\eta+\lambda_\sigma\nu)e^{i\mathbf{Q}\cdot\mathbf{R}_i}], \tag{20}$$

where m, η, and ν are order parameters, and $\lambda_\sigma=\pm 1$ for $\sigma=\uparrow,\downarrow$. The quasiparticles are given (up to constant energy shifts) by

$$E^{\pm}_{\mathbf{k}\alpha,\sigma}=\tfrac{1}{2}(\varepsilon_{\mathbf{k}+\mathbf{Q}}+\varepsilon_{\mathbf{k}})\pm\tfrac{1}{2}[(\varepsilon_{\mathbf{k}+\mathbf{Q}}-\varepsilon_{\mathbf{k}})^2+\Delta^2_\sigma]^{1/2}, \tag{21}$$

and $\mathbf{Q}=(\pi,\pi)$ is the nesting vector at $R=0$. The value of the gap at half-filling ($n_0=1$) is given by the effective interaction $\Delta_\sigma=\Delta=I_d\nu/2$ in the d-band case ($\Delta_\sigma=\Delta=I_s\nu/2$ in the s-band case).

The alternating magnetic order results in a two-sublattice magnetic structure and opens a gap Δ_σ for σ-spin electrons. Assuming the filling by n_0 electrons (per one band d sub-

band or s band), we analyze only the following commensurate magnetic phases: (i) ferromagnetic (FM), $m=\min\{n_0,2-n_0\}$, $\nu=\eta=0$; (ii) partial ferromagnetic (PFM), $m\neq 0$, $m<\min\{n_0,2-n_0\}$, $\nu=\eta=0$; (iii) antiferromagnetic (AFM), $\nu\neq 0$, $m=\eta=0$; and (iv) special ferrimagnetic (SFIM), $m=|1-n_0|$, $\nu\neq 0$, $\eta\neq 0$; here, the stability follows from the Fermi level lying within the gap between two majority Slater subbands.

In the region of their stability, the energies of magnetic phases are determined using the total energy expressions within the GHF approximation,

$$E(\{n_{i\alpha,\sigma}\})=E_{\mathrm{GHF}}+E_{\mathrm{corr}}, \tag{22}$$

where E_{GHF} is determined as in the HF approximation from the quasiparticle energies (21). For simplicity, we give only the formula for less than half-filling ($n_0\leqslant 1$),

$$E_{\mathrm{GHF}}=\frac{1}{N}\sum_{\alpha,\mathbf{k}\in K(\uparrow)} E^{-}_{\mathbf{k}\alpha,\uparrow}+\frac{1}{N}\sum_{\alpha,\mathbf{k}\in K(\downarrow)} E^{-}_{\mathbf{k}\alpha,\downarrow}-\langle H_{\mathrm{int}}\rangle, \tag{23}$$

where $K(\sigma)$ is a set of the occupied quasiparticle states $E^{-}_{\mathbf{k}\alpha,\sigma}$, Eq. (21), in the lower Slater subband for σ spin. The interaction energy $\langle H_{\mathrm{int}}\rangle$ is subtracted to avoid double counting, with the form of H_{int} determined by the used Hamiltonian, either H_s or H_d.

The correlation energy depends on the magnetic order, and is calculated using the local ansatz (18),[24,26]

$$E_{\mathrm{corr}}=\frac{\langle\Psi_0(\{n_{i\alpha,\sigma}\})|H_d|\Psi_0(\{n_{i\alpha,\sigma}\})\rangle}{\langle\Psi_0(\{n_{i\alpha,\sigma}\})|\Psi_0(\{n_{i\alpha,\sigma}\})\rangle}-E_{\mathrm{GHF}}. \tag{24}$$

In the s-band case we adopted the value of $E_{\mathrm{corr}}=0$, which is exact for the FM states, and avoids double counting of the correlation contributions in the PM and AFM states. The treatment of atomic correlations in the d band beyond the GRPA is only approximate, but suffices to get qualitative results for the magnetic phase diagrams reported below. These correlations vanish in the FM phase, but are finite in the PM state, and therefore the value of the Stoner parameter at the FM instability is found in an approximation. On the contrary, they have no influence on the lines of the AFM instabilities, where the order parameter ν increases continuosly from zero. Here we used the local approximation to evaluate the respective averages, when the exponentials in the wave functions $\Psi_0(\{n_{i\alpha,\sigma}\})$, Eq. (18), are expanded in Eq. (24). More details may be found in Ref. 24. The magnetic phase diagrams are next found using the instabilities of the nonmagnetic states, and by comparing the total energies (22) of the magnetic phases in the region of their stability.

As an illustrative example, we limit ourselves here to the 2D models (1) and (3) with nearest- (t) and next-nearest- (t') neighbor hopping. By changing the value of $R=2t'/t$, the bands (2) become flat in Γ-X and Γ-Y direction and the noninteracting susceptibilities $\chi^0(\mathbf{k},\omega)$ change. The singularity in the AFM susceptibility $\chi^0(\mathbf{Q},\omega)$ [$\mathbf{Q}=(\pi,\pi)$] moves to lower energies, as shown in Fig. 4, and gradually disappears, while the FM susceptibility $\chi^0(\mathbf{0},\omega)=N(\omega)$ develops a peak at low energies (see the inset of Fig. 4). Therefore, the RPA instabilities of the s-band model towards FM states occur at all electron densities (Fig. 5), and are enhanced at low n for increasing t'.[7] One finds that these instabilities occur towards the saturated FM states (with a maximum value of $m=|1-n_0|$) in most cases. As expected, the AFM (SFIM) order is more stable near half-filling.

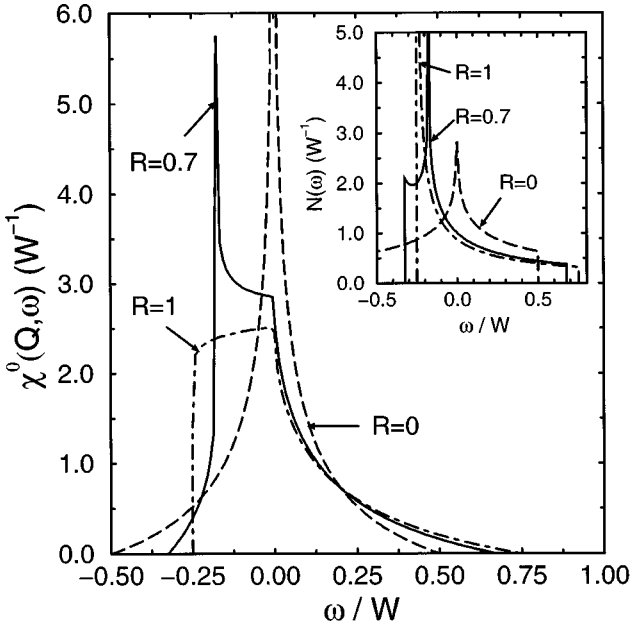

FIG. 4. Free susceptibility $\chi^0(\mathbf{Q},\omega)$ as obtained at the nesting vector $\mathbf{Q}=(\pi,\pi)$ for the 2D densities of states with $R=0$, 0.7, and 1.0 ($W=8t$). The corresponding densities of states $N(\omega)$ are shown in the inset.

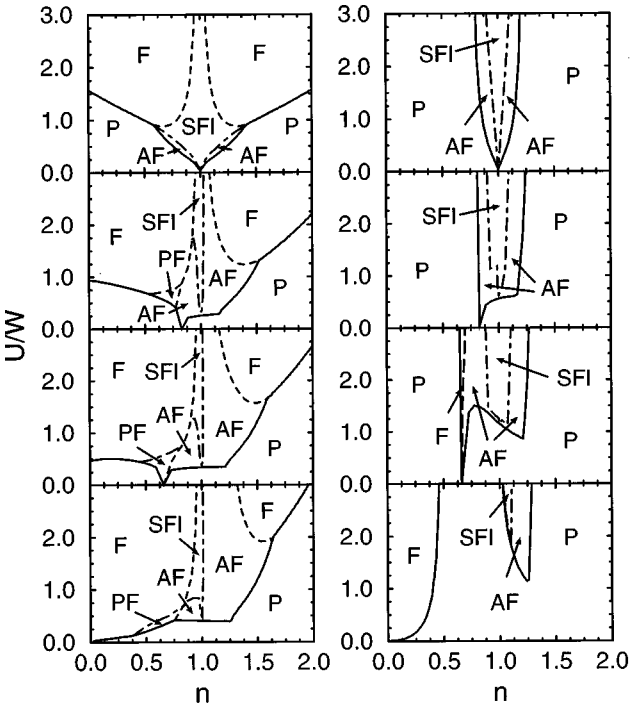

FIG. 5. RPA (left) and GRPA (right) phase diagrams for the s-band case and for $R=0$, 0.4, 0.7, and 1.0 from top to bottom. Solid lines give the instabilities with increasing U of paramagnetic (P) to ferromagnetic (F) or antiferromagnetic (AF) states. The special ferrimagnetic states (SFI) are separated by dot-dashed lines. Ferromagnetic states are saturated (F) except for small regions in the three lowest panels to the left (PF).

If correlation effects (renormalization of U within the GRPA) are included, the phase diagrams change drastically (Fig. 5). The FM instability disappears almost entirely in the GRPA if $R<1$, except just in a narrow region around the VHS for larger values of R. At $R=0$ it is suppressed at any n, in agreement with Rudin and Mattis.[30] As also no instability of the PM state towards the FM order is found in infinite dimension,[21] it is likely that it does not exist in hypercubic lattices at $R=0$.[31] The situation changes when particle-hole symmetry is broken for $t'>0$, and the FM order is stabilized by infinitesimal U at the VHS point, if $R>0.55$.[15] Remarkably, at $R=1$ *ferromagnetism is stable at low density*, $n<0.45$, as a consequence of flat-band behavior, $\varepsilon_{\mathbf{k}}=-2t$, if $\mathbf{k}=(k_x,0)$ or $\mathbf{k}=(0,k_y)$.

The AFM order is found to be more robust and exists around half-filling at any value of $R\leqslant 1$, with electron correlations included. In agreement with expectations, the region of AFM order at intermediate values of $U/W\geqslant 1.0$ expands when the kinetic energy in the ordered state increases with the increasing intrasublattice hopping t', both in the RPA and in the GRPA, as shown in Fig. 5. On the contrary, at $R=1$ the region of antiferromagnetism is much reduced compared with $R=0$. It is expected that incommensurate magnetic order with AFM correlations is stable in between the AFM and PM phases, as shown recently within this method in infinite dimensions.[21,32]

In contrast to ferromagnetism, the tendency towards AFM order at and near half-filling is weakened by the increasing next-nearest-neighbor hopping t', as the shape of the Fermi surface changes and the perfect nesting condition is not satisfied. At $R=0$, the transition to the AFM state occurs at infinitesimal $U>0$, and the magnetic moment ν increases gradually from zero with increasing U. This behavior is characteristic of perfect nested band structures, and is replaced by a jump to a finite magnetization ν which occurs at finite $U>0$, if $R>0$. With increasing R the lower quasiparticle subband $E^-(\mathbf{k})$, Eq. (21) becomes more flat and it is gradually more difficult to stabilize an AFM state. Therefore, the critical value of the Coulomb interaction U_c/W, increases with increasing R, as shown in Fig. 6.

It is interesting to ask whether the insulating AFM state at half filling and $R=0$ is replaced by itinerant antiferromagnetism with increasing values of t'. The gap in the AFM state at the transition point is determined by the energy difference between the top of the lower Slater subband E^- at $\mathbf{k}=(\pi/2,\pi/2)$ and the minimum of the upper Slater subband E^+ at $\mathbf{k}=(\pi,0)$. Using the effective Coulomb interaction $\overline{U}$, we find that the AFM state is always insulating at the transition point, except at $R=1$, where the gap between the Slater subbands closes and the AFM state is weakly metallic, as shown in Fig. 6. The onset of metallic behavior occurs in GRPA at $2t'=\Delta$, where $\Delta_\sigma=\Delta=I_s\nu/2$ in Eq. (21). If $R=1$, one finds at the transition point $\overline{U_c}=0.409W$, and $\nu=0.606$, and the splitting $\Delta=0.124W$, just somewhat smaller than $2t'=0.125W$. This results in a very small difference of the energies, $\Delta E=E^+(X)-E^-(S)=-2.2\times10^{-3}W$, and supports the recent conclusion of Duffy and Moreo[33] that itinerant magnetism is difficult to realize in the U-t-t' Hubbard model, without the second-neighbor hopping t'' along the x and y directions. Morever, it seems that the

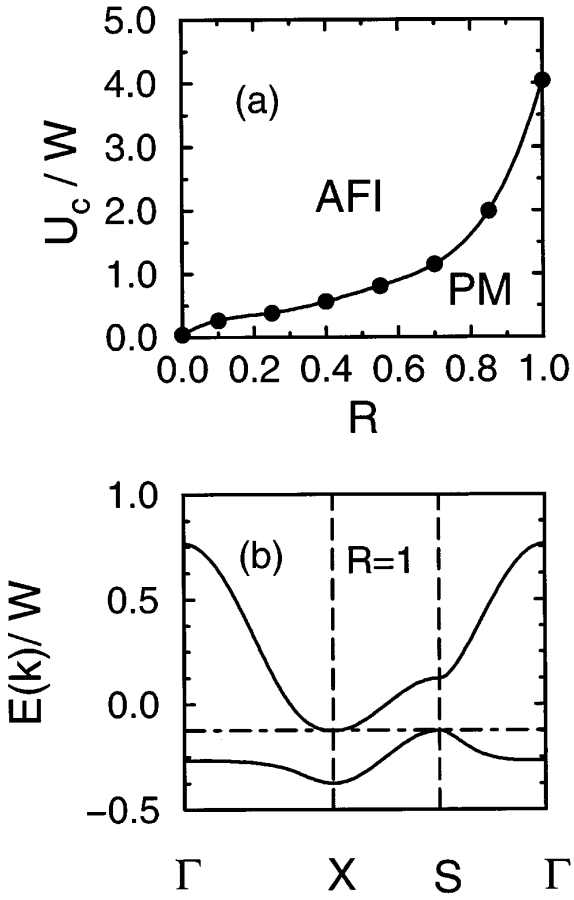

FIG. 6. Instability of a paramagnetic metallic (PM) to antiferromagnetic insulating (AFI) ground state at half-filling ($n=1$) in the Hubbard model (1): (a) critical value of the Coulomb interaction U_c as function of $R=2t'/t$, (b) electronic structure in an almost insulating (weakly metallic) AFM state obtained at $U=4.04W$ and $R=1$.

critical values of U obtained for the onset of AFM long-range order (LRO) might be overestimated at finite R, as we find the AFM instability at $U_c\simeq 4.5t$ for $R=0.4$, while the quantum Monte Carlo calculations suggest a value $U_c\simeq 2.5t$.[7,33] However, they agree with the metal-insulator transition estimated to be somewhere in the range of $4t<U_c<6t$, if $R=0.4$.

The RPA phase diagram of the d-band model is similar to that of the s-band model (Fig. 7), but the SFIM phase is destabilized by the interorbital exchange interaction J, and thus the AFM state is found instead in a broader range of parameters. As a consequence of the weaker screening by particle-particle diagrams (12), the conditions for FM LRO are less restrictive,[34] and the FM instabilities occur in the GRPA at any value of R, but for larger interactions (Fig. 7). As in the s-band case, FM order is favored at low electronic filling for $0.4<R<1.0$ due to weaker dispersion. As already seen in the screening of the Stoner parameter I_d, the spin-spin correlations restrict the region of FM states, in particular at $R=0$, and for $n>7.5$, if $R\geqslant 0.4$. Furthermore, one finds that weak ferromagnetism is somewhat more pronounced than in the s band and survives for the screened interactions, but occurs only in a relatively narrow range of n. This shows that partly polarized FM states are more likely to result from

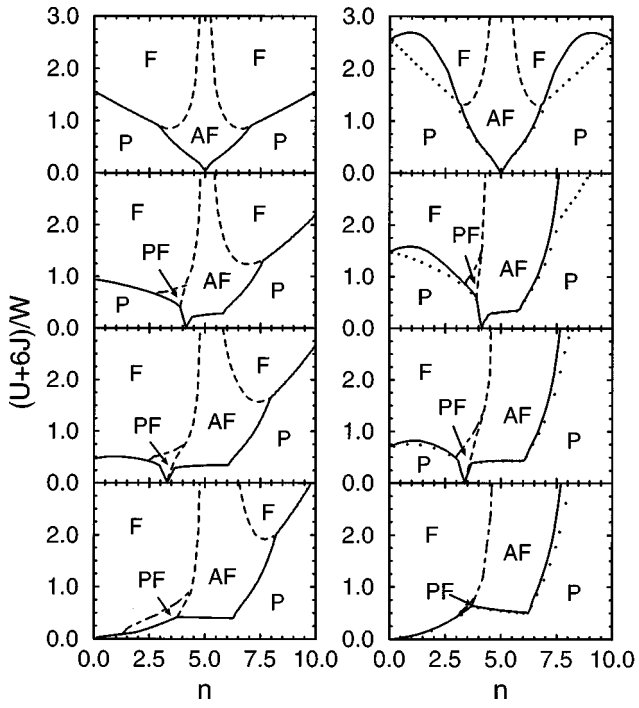

FIG. 7. The same as in Fig. 5, but for the d-band model (2) with $J/U=0.25$. The magnetic instabilities are shown by solid lines, while dotted lines indicate the same instabilities if the spin-spin correlations are neglected.

either the local maxima or the splittings between e_g and t_{2g} orbitals in realistic band structures of $3d$ transition metals.

IV. SUMMARY AND CONCLUSIONS

Summarizing, we conclude that the FM states are stable not only at, but also in the neighborhood of the VHS in the s-band model, if the band filling n is small. This suggests that ferromagnetism might be realized in the Hubbard model also in three dimensions, but only if the particle-hole symmetry is broken and the kinetic energy satisfies rather *extreme* conditions. Therefore, the s-band model cannot serve as a generic description of itinerant magnetism in transition metals. Instead the orbital degeneracy of the d states is crucial to explain magnetic states, and the interorbital exchange coupling J plays an important role.

Although no more than qualitative statements can be made for realistic transition metals, it is interesting to compare the obtained phase diagrams with the known interaction parameters of $3d$ systems. The values of U and J are approximately known for $3d$ transition metals and may be obtained from the multiplet splittings, as discussed in detail by van der Marel and Sawatzky.[22] This analysis leads to $U=2.55$, 2.76, and 2.97 eV, for Fe, Co, and Ni, respectively, while the values of J are given by the same ratio $J/U=0.27$.[23] These values of U are close to those considered by one of us in an earlier study of ferromagnetism in $3d$ metals,[23] and we treat them here as representative ones. Taking the bandwidths of Fe, Co, and Ni as determined by Andersen, Jepsen, and Glötzel,[35] $W=5.43$, 4.84, and 4.35 eV, respectively, this results in the HF values of the magnetic interaction for these elements of $(U+6J)/W=1.23$, 1.49, and 1.79, respectively. We assumed the electron filling of $n=7.3$, 8.3, and 9.4 in the d band and $R=0$ in our model (3) to simulate qualitatively the situation in Fe, Co, and Ni, and found a reduction of the respective Stoner parameter due to particle-particle renormalization and the spin-spin correlations of the order of $I_d/I_{\mathrm{HF}}\simeq 0.61$, 0.58, and 0.54, respectively. Interestingly, these values are almost constant as the increasing values of $(U+6J)/W$ are counterbalanced by the smaller reduction of I_d (both by particle-particle and even more by spin-spin correlations) when the electronic filling increases towards the filled band. Taking $J/U=0.25$ in a realistic model with canonical d bands,[26] one finds instead that $I_d/I_{\mathrm{HF}}\simeq 0.63$, 0.57, and 0.52. The agreement is very good indeed granted the simplicity of the model.

Furthermore, using the values of I_d derived above and realistic values of d-band widths,[35] one finds the Stoner parameters $I_d\simeq 0.72$, 0.82, and 0.92 eV for Fe, Co, and Ni, respectively. These values are significantly lower than those deduced by Gunnarsson from the local-density approximation (LDA) calculations, being 0.92, 0.99, and 1.01, respectively.[36] In spite of the qualitative nature of this comparison, this allows us to conclude that important corrections of the Stoner parameter exist due to nonlocal electron correlation effects, as in particular due to the spin-spin interorbital correlations, which cannot be dealt with in the standard band structure calculations based on the LDA. Thus, in spite of some attempts which exist in the literature,[37] there is no way to deduce reliable values of the Stoner parameter from band structure calculations performed within the LDA.

An additional factor which might stabilize ferromagnetism in the d-band model is the flattening of the bands with increasing values of R. Then magnetic states are possible even for rather small interactions U. Of course, this tendency is overemphasized in the present 2D model by the Van Hove singularity, but it is expected that strong next-nearest-neighbor hopping t' may lead to FM instabilities also in three-dimensional or quasi-2D systems at low filling. It would be interesting to verify this prediction, if such materials could be synthesized.

Altogether, we have shown that a correct quantitative description of ferromagnetism in transition metals is only possible within a realistic d-band model (3), and when the particle-particle screening and spin-spin correlations are included. In order to obtain more quantitative results, however, realistic densities of states have to be used. A somewhat different situation, however, is found for the AFM states, where band structure effects (like perfect nesting) dominate, at least at weak and intermediate values of U, and the s-band model might then suffice to explain qualitatively the experimental data for AFM Cr and its alloys.[21]

ACKNOWLEDGMENTS

We thank Richard Hlubina and Gernot Stollhoff for stimulating discussions. A.M.O. acknowledges partial support by the Committee of Scientific Research (KBN) of Poland, Project No. 2 P03B 144 08.

*Permanent address: Institute of Physics, Jagellonian University, Reymonta 4, PL-30059 Kraków, Poland.
[1] J. Hubbard, Proc. R. Soc. London, Ser. A **276**, 238 (1963); M. C. Gutzwiller, Phys. Rev. Lett. **10**, 159 (1963).
[2] Y. Kanamori, Prog. Theor. Phys. **30**, 275 (1966).
[3] A. M. Oleś, J. Phys. C **15**, L1065 (1982).
[4] W. von der Linden and D. M. Edwards, J. Phys., Condens. Matter. **3**, 4917 (1991).
[5] T. Hanisch and E. Müller-Hartmann, Ann. Physik **2**, 381 (1993); P. Wurth and E. Müller-Hartmann, *ibid.* **4**, 145 (1995).
[6] J. E. Hirsch, Phys. Rev. B **40**, 2354 (1989); M. Kollar, R. Strack, and D. Vollhardt, *ibid.* **53**, 9225 (1996); J. C. Amandon and J. E. Hirsch, *ibid.* **54**, 6364 (1996).
[7] H. Q. Lin and J. E. Hirsch, Phys. Rev. B **35**, 3359 (1987).
[8] A. Mielke, Phys. Lett. A **174**, 443 (1993); A. Mielke and H. Tasaki, Commun. Math. Phys. **158**, 341 (1993).
[9] H. Tasaki, Phys. Rev. Lett. **69**, 1608 (1992); **75**, 4678 (1995).
[10] E. Müller-Hartmann, J. Low Temp. Phys. **99**, 349 (1995).
[11] K. Penc, H. Shiba, F. Mila, and T. Tsukagoshi, Phys. Rev. B **54**, 4056 (1996).
[12] P. Pieri, S. Daul, D. Baeriswyl, M. Dzierzawa, and P. Fazekas, Phys. Rev. B **54**, 9250 (1996).
[13] L. M. Falicov and R. H. Victora, Phys. Rev. B **30**, 1695 (1984).
[14] G. M. Pastor, R. Hirsch, and B. Mühlschlegel, Phys. Rev. Lett. **72**, 3879 (1994); Phys. Rev. B **53**, 10 382 (1996).
[15] R. Hlubina, S. Sorella, and F. Guinea, Phys. Rev. Lett. **78**, 1343 (1997).
[16] A. M. Oleś and P. Prelovśek, Phys. Rev. B **43**, 13 348 (1991).
[17] L. Chen, C. Bourbonnais, T. Li, and A. M. S. Tremblay, Phys. Rev. Lett. **66**, 369 (1991).
[18] N. E. Bickers, D. J. Scalapino, and S. R. White, Phys. Rev. Lett. **62**, 961 (1989).
[19] N. E. Bickers and D. J. Scalapino, Ann. Phys. (N.Y.) **193**, 206 (1989).
[20] N. Bulut, D. J. Scalapino, and S. R. White, Phys. Rev. B **47**, 2742 (1993).
[21] J. K. Freericks and M. Jarrell, Phys. Rev. Lett. **74**, 186 (1995).
[22] D. van der Marel and G. A. Sawatzky, Phys. Rev. B **37**, 10 674 (1988).
[23] G. Stollhoff, A. M. Oleś, and V. Heine, Phys. Rev. B **41**, 7028 (1990).
[24] A. M. Oleś, Phys. Rev. B **28**, 327 (1983).
[25] L. P. Kadanoff and G. Baym, *Quantum Statistical Mechanics*, Advanced Book Classics (Addison-Wesley, Reading, MA, 1989).
[26] G. Stollhoff, J. Chem. Phys. **105**, 227 (1996).
[27] The intraorbital (particle-particle) correlations were described by the local ansatz (18) in Ref. 23.
[28] The correlation energy gained by spin correlations is largest at half-filling and vanishes if $n \to 0$.
[29] D. R. Penn, Phys. Rev. **142**, 350 (1966).
[30] S. Rudin and D. C. Mattis, Phys. Lett. **110A**, 273 (1985).
[31] The absence of FM instability in the presence of correlation effects does not suffice to conclude that ferromagnetism does not occur at any density and U. As shown in Refs. 4 and 5, the FM g.s. is locally stable in a 2D Hubbard model near half-filling at $U \to \infty$.
[32] A. N. Tahvildar-Zadeh, J. K. Freericks, and M. Jarrell, Phys. Rev. B **55**, 942 (1997).
[33] D. Duffy and A. Moreo, Phys. Rev. B **55**, R676 (1997).
[34] It is well known that ferromagnetism in transition metals is promoted by the Hund's rule exchange J. Its mechanism is, however, different from that pointed out by Kugel and Khomskii for transition metal oxides [K. I. Kugel and D. I. Khomskii, Sov. Phys. Usp. **25**, 231 (1982)]. While local moments form in partially filled orbitals of transition metals, a particular orbital ordering suppresses the antiferromagnetic superexchange and promotes weak ferromagnetic interactions between Cu^{2+} ions in $KCuF_3$.
[35] O. K. Andersen, O. Jepsen, and G. Glötzel, *Highlights of Condensed Matter Theory*, LXXXIX Corso Societa Italiana di Fisica (Tipografia Compositori, Bologna, 1985), p. 59.
[36] O. Gunnarsson, J. Phys. F **6**, 587 (1976).
[37] L. Severin, M. S. S. Brooks, and B. Johansson, Phys. Rev. Lett. **71**, 3214 (1993); **76**, 856 (1996); **76**, 3466(E) (1996); G. Stollhoff, A. M. Oleś, and V. Heine, *ibid.* **76**, 855 (1996).